To the Editor:

The feedback-block-oriented models were introduced by M. Pottmann and R. K. Pearson in "Block Oriented NARMAX Models with Output Multiplicities," (Jan. 1998) to the development of NARMAX models for processes exhibiting output multiplicities. The aim of their work was to design a model structure that permits the steady-state behavior to be specified independently of the process dynamics. The proposed models were suggested to be suitable for gray-box modeling approaches where it is assumed that the steady-state behavior of the process is known. The generated structures were shown to be the addition to the family of block oriented models, of which the two most popular members are Wiener and Hammerstein models.

The main difference between these popular block-oriented models and the proposed "feedback-block-oriented" model is that the process dynamics cannot be specified independently of the steady state in the case of "feedback-block-oriented model," although the steady-state behavior is defined independently of process dynamics.

In this letter, the drawbacks of this effect and a small simulation example are presented in order to show that care must be taken in the application of this model structure. The equivalent NARMAX representation of the simplest feedback-block-oriented model (Structure I) is

$$y(k) = F[z(k)] = \sum_{i=1}^{p} a_i y(k-i) + \sum_{j=1}^{q} b_j\{u(k-j) + N[y(k-j)]\} \quad (1)$$

where $z(k) = [y(k), \ldots, y(k - \max(p,q)), u(k), \ldots, u(k-q)]$ denotes the state vector consisting of the scalar output and input sequence, and $N(.)$ denotes the function of the steady-state nonlinearity, respectively.

By the linearization of the nonlinear model at a given state, $z(k)$, which is not necessary equilibrium, the following linear time invariant model can be obtained in each operating point

$$y(k) = \sum_{i=1}^{\max(p,q)} a_i^* y(k-i) + \sum_{j=1}^{q} b_j^* u(k-j) + c \quad (2)$$

where

$$a_i^* = \frac{\partial F(z(k))}{\partial y(k-i)} = a_i + b_i \frac{\partial N[y(k-i)]}{\partial y(k-i)}$$

$$b_j^* = b_j = \frac{\partial F(z(k))}{\partial u(k-j)}$$

$$i = 1, \ldots, \max(p,q) \qquad j = 1, \ldots, q \quad (3)$$

where

$$c = z(k) - \sum_{i=1}^{\max(p,q)} a_i^* y(k-i) + \sum_{j=1}^{q} b_j^* u(k-j).$$

The previous equation shows that the steady-state nonlinearity has effect on the process dynamic through the derivation of the function $N[y(k-i)]$. Therefore, during the identification of the $\{a_i\}$ and $\{b_i\}$ parameters of the gain-independent linear dynamic model, not only the process dynamic should be described, as in the case of the Wiener and Hammerstein model, but the identified dynamic model should also compensate this effect.

In some cases this could be very difficult, because the poles of discrete-time models that emerge from a correctly sampled, continuous system cannot be situated everywhere in the complex plane. The coefficients of the linearized model has to satisfy (Tulleken, 1992)

$$(-1)^{i+1} a_i^* \geq 0 \quad (4)$$

From Eq. 3, it can be seen that this constraint could not be fulfilled in the case of some nonlinearities.

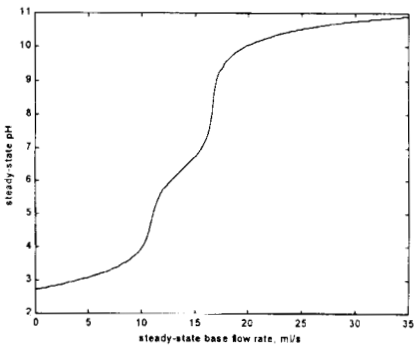

Figure 1. Steady-state characteristic.

The feedback-block-oriented models can be used for modeling nonlinear processes without steady-state multiplicities. Therefore, in order to demonstrate the mentioned problem, a simple realistic simulation example is presented where the proposed approach is applied to a pH neutralization plant (Henson and Seborg, 1997). This example is often used as a case study for block-oriented modeling and model-based control, because the steady-state and the first-order dynamic behavior can be easily separated.

From the steady-state behavior (the titration-curve) (Figure 1), the function $\partial N(y)/\partial y$ can be calculated (Figure 2). The dynamic behavior of the process can be calculated from the resident-time

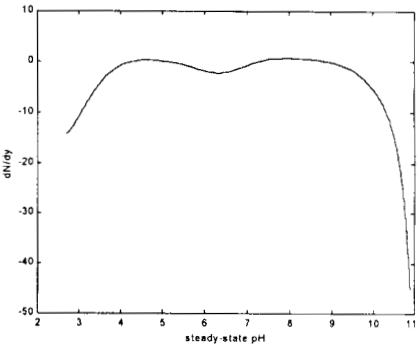

Figure 2. Derivative of the $N(.)$ function.

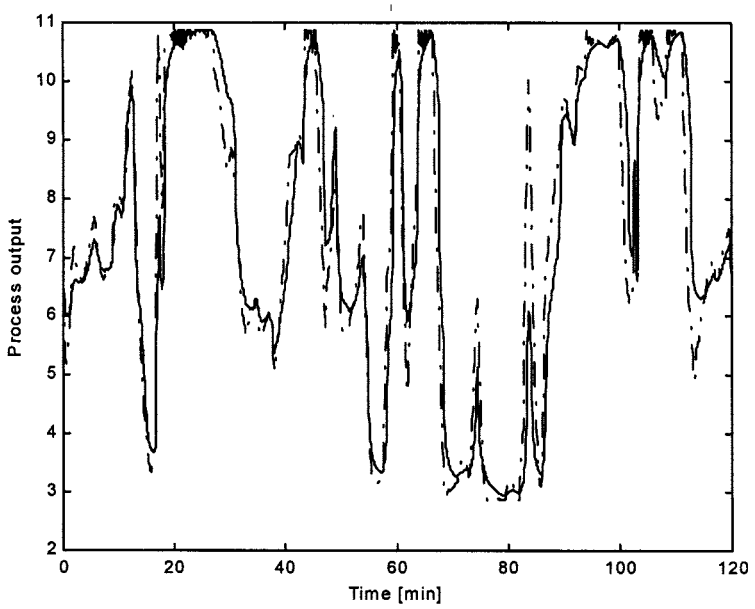

Figure 3. Simulation results (—— real plant, —·— block-oriented model).

$a_1^* = \exp(-T_0/\tau) = [0.92 - 0.97]$, where $\tau = [55 - 169]$ s, is the resident time and $T_0 = 5$ s is the discrete sampling time. As Figure 2 and Eqs. 3 and 4 show, it is impossible to get reliable dynamic model parameters with unity gain for the whole pH range. As Figure 3 shows after the identification of the unity gained dynamic model, the performance of the feedback-block-oriented model was not satisfactory, even if the linear dynamic is replaced by linear multimodels (Johansen, 1994), where its operating range is represented by fuzzy sets. For the compensation of the effect of the steady-state nonlinearity to the dynamic, the operating regimes of the local linear models have to be determined in the range of the pH, although it should be the function of the base flow rate only. Therefore, in some cases getting a feedback-block-oriented model with linear dynamic multimodels could be a more complex task then getting a pure NARMAX model represented by a local linear modeling framework.

Based on the proposed considerations, it can be stated that care must be taken in the application of the feedback-block-oriented model, because, in the case of some nonlinearities, an extreme price may be paid for imposing this structurally and analytically convenient restriction on a NARMAX model.

Literature cited

Henson, M. A., and D. E. Seborg, "Adaptive Input-Output Linearization of a pH Neutralisation Process," *Int. J. of Adaptive Control and Signal Processing*, **11**, 171 (1997).

Johansen, T. A., "Operating Regime based Process Modeling and Identification," PhD Thesis, The Norwegian Institute of Technology, (1994).

Pottmann, M., and R. K. Pearson, Block-Oriented NARMAX Models with Output Multiplicities, *AIChE Journal*, Vol. 44, No. 1, 131–140, 1998.

H.J.A.F. Tulleken, Grey-box Modelling and Identification Topics, Ph.D. thesis, Delft University of Technology, 1992.

J. Aboni, L. Nagy, and F. Szeifert
Dept. of Chemical Engineering Cybernetics
University of Veszprém
H-8201, Veszprem, Hungary

Reply:

In their discussion of our article, Abonyi, Nagy, and Szeifert make a number of observations with which we agree, and other observations with which we differ. Certainly, we agree with their final conclusion that "care must be taken in the application of the feedback-block-oriented model," a caution that we would extend to *all* approximate model classes.

Conversely, we disagree with the suggestion that the process dynamics and the steady-state behavior *can* be specified independently for the more common Wiener and Hammerstein models. For example, if we compare the response of the Hammerstein and Wiener models based on the same static nonlinearity and the same linear dynamic model, and if the steady-state gain of the linear model is taken to be 1, the static nonlinearity completely determines the steady-state behavior and both models have identical linearized dynamics. The only difference, then, arises in their transient behavior, and these differences can be profound (Pearson, 1995). As a specific example, compare the impulse responses of the Hammerstein and Wiener models formed from the first-order linear model

$$y(k) = \alpha y(k-1) + (1-\alpha)u(k-1) \tag{1}$$

and the quadratic nonlinearity

$$f(x) = x + \gamma x^2. \tag{2}$$

In the Hammerstein model, the effect of the static nonlinearity is to simply scale the impulse input from amplitude λ to amplitude $\lambda = \gamma\lambda^2$ and, for fixed λ, the overall model response is indistinguishable from that of a first-order linear model. Conversely, the response of the Wiener model to the same input is easily computed to be

$$y(k) = (1-\alpha)\lambda\alpha^k + \gamma(1-\alpha)^2\lambda^2\beta^k, \tag{3}$$

where $\beta = \alpha^2$. For fixed λ, note that this impulse response is indistinguishable from that of a *second-order* linear model. We would therefore argue that, exactly as in the case of the feedback block-oriented structures, the process dynamics *cannot* be specified independently of the steady state.

Furthermore, we disagree with the notion that the linear model parameters in the feedback block-oriented model need to compensate for the static nonlinearity. In contrast, we view this interconnection between linear dynamics and static nonlinearity as a desirable and necessary feature which makes the proposed block-oriented model applicable to processes which exhibit *both* static nonlinearities *and* operating-point dependent dynamics (with output multiplicity as an extreme form of this general type of behavior). As an example without output multiplicities, consider high-purity distillation columns, for which the apparent time constant associated with top composition changes

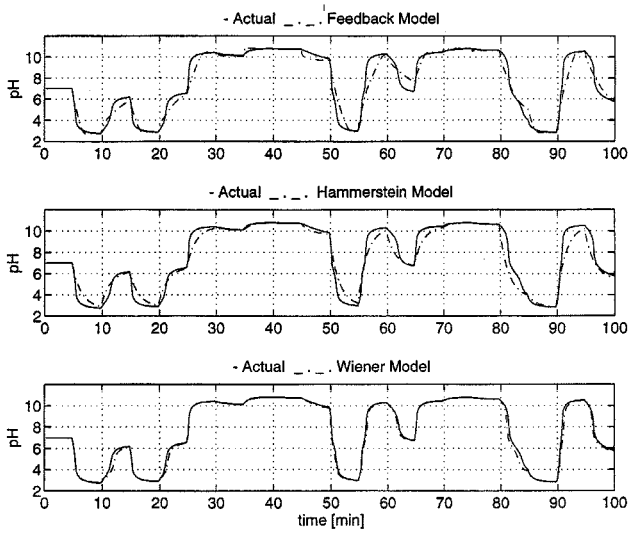

Figure 1. Comparison of block-oriented models for the pH neutralization process.

significantly with reflux flow (Eskanat et al., 1991). For this type of process, feedback block-oriented models can-due to the interactions between static characteristic and model dynamics-significantly outperform both Hammerstein and Wiener models, as discussed in detail elsewhere (Pearson and Pottman, 1999).

Abonyi, Nagy, and Szeifert also mention a criterion of Tulleken that the linearization of our feedback block-oriented model does not obviously satisfy. In fact, this criterion is a stability condition [Tulleken, 1992], motivated by the starting assumption that the continuous-time model being approximated is open-loop stable. As Tulleken himself notes in the discussion of that criterion, exothermic chemical reactors like the one we consider in our article are not open-loop stable (specifically, the second of the three steady states is unstable). Consequently, this stability criterion for the linearized model should *not* be satisfied at every local operating point. The question of where along the steady-state locus this condition is or is not satisfied is an interesting one, however, and might provide some useful insights into the transition dynamics discussed in the summary of our article or into the issue of model order selection (that is, choice of the dynamic order parameters p and q in the linear ARMAX model on which the feedback block-oriented model is based).

With regard to the simulation example presented by Abonyi et al., we are not surprised by the unsatisfactory performance of the feedback block oriented model, because the process considered inherently has a Wiener type structure, so we would expect the Wiener model to be more appropriate. In order to provide a basis for comparison, we developed for the same process, a set of Hammerstein, Wiener, and feedback block-oriented models with simple first-order dynamics. The results shown in Figure 1 indicate that the performance of the feedback block-oriented model is quite similar to that of the Hammerstein model (neither of these model structures are particularly well suited to this process), and both models are highly inferior to the Wiener model.

Finally, it is important to re-emphasize that we approach empirical modeling as a process of approximation and, as a consequence, there can be no "correct" empirical model. Different choices of model structure and identification algorithm can be expected to yield different approximations, each with its own associated strengths and weaknesses. In our view, the greatest strengths of the feedback block-oriented model structure are, first, that is permits an exact match of known steady-state characteristics, secondly, that, once these steady-state characteristics are fixed, the subsequent parameter estimation problem is straightforward, and finally, that it is capable of exhibiting significantly different types of dynamic behavior than either Wiener or Hammerstein models.

Literature cited

Pearson, R. K., "Nonlinear Input/Output Modeling," *J. Proc. Control*, **5**, 197 (1995).
Eskinat, E., S. H. Johnson, and W. L. Luyben, "Use of Hammerstein Models in Identification of Nonlinear Systems," *AIChE J.*, **37**, 255 (1991).
Pearson, R. K., and M. Pottman, "Gray-box Identification of Block-oriented Nonlinear Models," *J. Process Control*, in press (1999).
Tulleken, H., "Gray-box Modelling and Identification Topics," PhD Thesis, Delft University of Technology, The Netherlands (1992).

Martin Pottmann
DuPont DACRON
Cape Fear Site
Wilmington, NC 28402

Ronald K. Pearson
Institut für Automatik
ETH Zürich
CH-8092 Zürich, Switzerland

To the Editor:

In a recent article by Matthews and Rawlings (May, 1998), three types of on-line experimental responses (viz., time variations of crystallizer temperature, slurry transmittance, and solution density) from a 3-L glass, jacketed, agitated, and seeded batch crystallizer were used for model identification. The optimal parameter estimates were selected at the maximum of the Bayesian posterior probability density function and, also, the simultaneous minimum of the objective function (Eq. 9). The errors, that is, the difference between actual and model predicted values in measured variables at sampling times, are assumed to be independent, unbiased, and normally distributed with zero mean and finite covariance matrix. Thus

$$e_{ki} = y_{ki} - f_{ij}(x_k, \theta_{ij}) \quad i = 1, 2, \ldots n_k \quad k = 1, 2, 1 \ldots m \quad (1)$$

where e_{ki} is the error of the ith observation of the kth variable, n_k is the number of observations made for the kth variable, m is the total number of measured variables, and θ_j is the model parameter. Scaling often influences the performance of most optimization techniques, and the normalized residuals are generally satisfactory.

In their initial model formulation, the authors used batch population and mass balance incorporating power law growth and nucleation kinetics in relative supersaturation, and attempted to infer the kinetic model parameters from observed experimental responses. I am concerned with the use of the Beer-Lambert law for relating the measured transmittance to the second moment of the crystal-size distributions. The transmittance can be directly related to the

projected surface area, but not the total surface area that can be determined from the second moment of the CSD. The arbitrary definitions of the initial and boundary conditions require additional qualification. The continuity between the seed and nuclei population density functions is implicitly assumed, although in reality the discontinuity will prevail at $L = 0$. The choice may be questionable of the initial seed mass and temperature as significant process variables for differentiating the designs of the identification experiments and gaining the maximum possible dynamic information in data over the duration of the experiment. Naturally, the resulting transmittance and concentration residuals for most runs would be large and scattered, as the model description would be inadequate. Although the seeding was effected at high levels of supersaturation in order to prevent the dissolution of the small seed loads, and both seed loading and temperature profiles were varied for different experiments, they seem not to significantly affect the process over the range. The variations of the dominant variable, that is, the relative supersaturation ratio S, were not evaluated. The simulated relative supersaturation profile in Figure 14 showed the initial rapid decay, remained at a low plateau over most of the batch time, and, finally, passed through a small peak prior to the end of the run. It is not clear how the relative supersaturation was produced and constrained between 0 and 1. The optimum temperature profiles were designed by posing a nonlinear program to identify piecewise linear temperature values that minimize either the determinant or the normalized trace of the inverse of the Gaussian Hessian matrix. With these optimal temperature profiles, the concentration profiles appeared to decay more slowly initially, then more rapidly over a short period, and, finally, approaching equilibrium value at a slower rate, thus achieving a more distinct sigmoidal shape than that in nonoptimal runs. The concentration decay rate passes through the maximum probably at the point of inflection. The concentration and transmittance data can be interrelated through their Eqs. 2 and 5.

The transmittance data relating to crystal surface area were not well described by the initial (inappropriate) model, as the residuals using the parameter estimates for the standard power law kinetic equations (Eqs. 3 and 4) from both the transmittance and concentration data were unacceptably large. The authors assumed that the results were not meaningful and proposed revisions in the model formulation. They incorporated two additional features, viz., dynamic shape factors in terms of aspect ratios and a power-law term of minimum crystal size in the revised size-dependent secondary nucleation rate model. They defined the area and volume shape factors in terms of aspects ratios (that is, length-to-width l_w and depth-to-width ratio d_w) to describe the seed crystal habit. They assumed that the minimum crystal size that is required for effective participation in secondary nucleation processes would be an important model parameter. Inclusion of such additional features on an *ad hoc* basis may lose the generic character of the model and change the model description. Thus, seven model parameters were estimated using a proposed scheme from all the available concentration, transmittance, and optical microscope data that were obtained in a series of eleven crystallization experiments. Also, the improved closure between the observed and calculated values for the transmittance data was demonstrated in the revised model. As a general observation in most parameter estimation procedures, the closure improves at the expense of complexity with the number of the parameters and the precision of the model parameters is generally indicated by the confidence interval. The covariance matrix of the probabilitly distributions can provide a measure of the reliability of the estimates. In addition to the statistical inference about the parameter observability, the process controllability, and the model discrimination, the physics of the process supported by strong mechanistic corroboration is vitally important in selecting the appropriate types of experimental responses and the number of parameters in the model for its subsequent adequacy.

The essence of effective characterization of crystallization kinetics and their successful application in crystallizer design, control, and analysis resides in the recognition that all the kinetic events are rate processes. Although several kinetic events are identifiable in a crystallizer operation, crystallization kinetics in the literature are conventionally characterized in terms of two dominant rate processes occurring in a process of crystallization from solution, namely, crystal nucleation and growth. The terms *rate* and *rate concept* need careful definitions. The overall linear growth rate (in Eq. 3) is specific with respect to crystal number. The consistent definition of linear overall crystal growth rate for a multiparticulate batch system, where the total number of crystals is changing, is the time rate of change of total length of all crystals per crystal and not the time rate of a crystal size. Similarly, the nucleation rate (in Eqs. 4 and 17) is the nucleation rate at a vanishingly close to zero size and is expressed as the number per mass of solvent per unit time (that is, no./kg s). At the outset, it is necessary to emphasize the distinction between *process rate* and *rate of change* while establishing the kinetic correlations as has been suggested in the analysis of multiphase reactor systems (see, for example, Bisio and Kabel, 1985). The process rate, as used in crystal nucleation or growth rate, is just a concept and is always important in process analysis. One does not measure process rate directly, but only arrives at its values by some combination of measurement and theory. The rate of change follows the dictionary definition as familiar from the calculus, has derivative character, and is subject to measurement.

Although a large fraction of efforts were directed toward developing rate models and analytical solutions for the rate processes, both by continuous (analytical) and discrete (numerical) mathematical methods, the crystallization literature of engineering practice is still largely based on experimental data yielding empirical correlations. These correlating equations have been relatively uninfluenced by theory, as most theoretical solutions in most cases provide no satisfactory guidance for their functional behavior. Most analytical solutions are subject to uncertainty arising primarily from simplification and idealization both in model formulation and evaluation. Uncertainty and imprecision in experimental data may arise not only from incomplete definition and control of experimental environment, but also from errors of measurement. Empirical observations along with the theoretical support provide a sound basis for correlating equations over wide range of variables.

Literature cited

Matthews, H. B., and J. B. Rawlings, "Batch Crystallization of a Photochemical: Modeling, Control, and Filtration," *AIChE J.*, **44**, 1119 (1998).

Bisio, A., and R. L. Kabel, *Scaleup of Chemical Processes*, Wiley, New York, pp. 77–116 (1985).

Narayan S. Tavare
Dept. of Chemical Engineering
University of Bradford
West Yorkshire BD7 1DP, U.K.

Reply:

We appreciate Professor Tavare's interest in and comments on the article by Matthews and Rawlings. We would like to reply to some of his comments.

As Professor Tavare comments, the Beer-Lambert law relates the transmittance of light to the projected surface area of the particles via

$$I/I_0 = \exp\left(-l\int_0^\infty f(L,t)\,A_p(L)\,Q(L)\,dL\right)$$

in which I/I_0 is the transmittance, l is the light transmission path length, $f(L,t)$ is the particle-size distribution in characteristic length L at time t, $A_p(L)$ is the projected area of a particle of size L, and $Q(L)$ is the light extinction efficiency factor; $Q(L)=2$ if one assumes Fraunhoffer diffraction. However, the expectation of the projected area of a randomly oriented, convex particle is one-fourth its surface area (van de Hulst, 1957). Therefore, in the case of a distribution of convex particles passing through a flow cell without significant alignment in the flow cell (random orientation), $A_p(L)=1/4\,k_a L^2$, in which k_a is the particle surface area shape factor. Substituting these expressions into the equation above relates transmittance directly to the second moment of the CSD and produces Eq. 5 in the article.

We do not see what is arbitrary about the initial and boundary conditions. We are using the standard ones (Randolph and Larson, 1988). The population balance given in Eq. 1 in the article is a first-order hyperbolic equation. It is satisfied in a time, length domain

$$(L,t)\in\Omega,\quad \Omega=(0,\infty)\times(0,\infty)$$

In order to have a well-posed problem, auxiliary conditions are required on the value of f on the boundary of Ω, which are the two rays $t=0$, $L\geq 0$ and $L=0$, $t\geq 0$. On the first ray, we specify the initial condition, which is the crystal-size distribution (seed CSD) introduced into the crystallizer at $t=0$. We mention in the article the difficulty of measuring $f_S(L)$ precisely. See also (Matthews, 1997), available at http://www.che.wisc.edu/~hbm/research.html for further discussion of the seed distribution.

On the second ray, we define the boundary condition, which is related to the nucleation rate of new crystals at size $L=0$. If particles are nucleated at rate $B(t)$, and grow at rate $G(L,t)$, then the appropriate boundary condition is

$$f(0,t)=\frac{B(t)}{G(0,t)}$$

in agreement with Eq. 5.11 in Professor Tavare's comprehensive book on crystallizer simulation and design (Tavare, 1995). If one is interested in deriving this boundary condition, it might be best to write the original population balance with an impulse source term of strength $B(t)$ at $L=0$ to account for nucleation of new particles at zero size

$$\frac{\partial f(L,t)}{\partial t}=-\frac{\partial G(L,t)f(L,t)}{\partial L}+B(t)\delta(L)$$

Integrating this equation across a vanishingly small interval containing the line $L=0$ and assuming $f(0^-,t)=0$ also produces $f(0^+,t)=B(t)/G(0,t)$.

Professor Tavare's comment on a discontinuity at $L=0$ requires clarification. Because the population balance in Eq. 1 is a hyperbolic PDE, it has characteristic lines in the (L,t) plane. In our case, the family of lines with slope $dL/dt=G$ are characteristic lines for the PDE. Discontinuities in the data on either boundary given above are transmitted into region Ω along these characteristic lines. Any difference in $f(L,t)$ at the origin ($L=t=0$) caused by a difference between the seed distribution ($f_S(L)$, $L=0$) and the initial nucleation rate ($B(t)/G(0,t)$, $t=0$) propagates into region Ω along the characteristic line emanating from the origin. But, the location and character of any discontinuities in the solution are governed by the specified behavior on the boundaries. Once those conditions are set, we cannot change any of the continuity properties of the solution.

Whether one prefers the classic (strict solution) PDE theory given in the article, or a more modern view admitting generalized functions and weak solutions, is a matter of taste and mathematical background, but we do not understand why the boundary conditions or the locations of discontinuities in $f(L,t)$ would be in doubt.

We agree with Professor Tavare that the relative supersaturation S is a key variable, because it appears as the driving force in the growth and nucleation rates (Eqs. 3–4). However, we routinely calculate S, and we plot its value in Figure 14. We plot the model prediction of the solution concentration $C(t)$ in many of the figures, because that is the measured variable, or the directly inferred variable given our densitometer and its calibration with standards. We could take the measured (or inferred) value of C and compute a corresponding S, but that is not a measured quantity and requires a model for the saturation concentration $C_{sat}(T)$. When fitting data to models, it is more reliable to plot model predictions vs. directly measured quantities, not model-dependent transformations of measured quantities.

The relative supersaturation is a simple nonlinear function of the solution concentration (state variable) and solution temperature (input variable), and we constrain it to lie between zero and one by simply adding that nonlinear constraint to our optimal control problem. More discussion of including this type of constraint in crystallization models is available (Matthews et al., 1996; Miller and Rawlings, 1994; Rawlings et al., 1992a,b).

After the initial model was demonstrated to be inadequate to explain the data, we postulated two extensions: (i) change in crystal shape with time, and (ii) secondary nucleation whose rate depends on the sizes of the colliding crystals. The first extension was supported by optical micrographs of the crystals and the second extension is supported by the cited work of Rousseau et al. and Kubota and Fujiwara. We also state in the conclusion that other mechanisms to explain the data are certainly possible, and model discrimination would be a good next step in habit prediction and secondary nucleation crystallization studies. Our results merely provide another iteration in the classical scientific method: hypothesize, experiment, compare, revise.

Finally, we seem to diverge on the definition of *linear overall growth rate*, which we presume is the variable G in our article. If we generalize slightly, in our model $G(L,t)$ is *the growth rate of crystals* of size L at time t. Given the deterministic model in this study, that is an appropriate interpretation of the microscopic, physical meaning of G. If we wish to compute the macroscopic "time rate of change of total length of all crystals per crystal," which seems to be Professor Tavare's preferred definition of G, that quantity is simply computed

$$\frac{d/dt\int_0^\infty f(L,t)\,L\,dL}{\int_0^\infty f(L,t)\,dL}=\frac{d\mu_1/dt}{\mu_0}$$

in which μ_i is the ith moment of the CSD. If G is independent of size, tak-

ing moments of the population balance, Eq. 1 produces

$$\frac{d\mu_1/dt}{\mu_0} = G$$

so these two ''definitions'' of G are equivalent in the model proposed in our study. However, if the growth is size dependent, obviously the two definitions would differ; our definition is a function of time and size, and the other is a function of only time. We prefer a microscopic interpretation of G, especially if we next consider growth rate fluctuations possibly due to fluctuating environmental conditions or random inherent crystal imperfections. In that case, G is modeled as a random variable, which again describes the fluctuating growth rate of a particular crystal in the ensemble. In this case, the expectation of the macroscopic ''time rate of change of total length of all crystals per crystal" would still be directly computable from a stochastic model simulation, and we don't see why that quantity would be confused with a particular crystal's growth rate. We require a microscopic statement of a crystal's growth rate in order to write a continuity equation for the particle density function in the deterministic case or to calculate a particle trajectory in the stochastic case. We do not see how the proposed definition of a macroscopic quantity can substitute for that required information.

Literature cited

Matthews, H. B., ''Model Identification and Control of Batch Crystallization for an Industrial Chemical System,'' PhD Thesis, University of Wisconsin-Madison (1997).

Matthews, H. B., Stephen M. Miller, and James B. Rawlings, ''Model Identification for Crystallization: Theory and Experimental Verification,'' *Powder Tech.*, **88**, 227 (1996).

Miller, Stephen M., and James B. Rawlings, ''Model Identification and Control Strategies for Batch Cooling Crystallizers," *AIChE J.*, **40**(8), 1312 (Aug. 1994).

Randolph, Alan D., and Maurice A. Larson, *Theory of Particulate Processes*, 2nd ed., Academic Press, San Diego (1988).

Rawlings, J. B., W. R. Witkowski, and J. W. Eaton, ''Modelling and Control of Crystallizers,'' *Powder Tech.*, **69**, 3 (1992).

Rawlings, James B., Chester W. Sink, and Stephen M. Miller, ''Control of Crystallization Processes,'' *Handbook of Industrial Crystallization*, Allan S. Myerson, ed., Butterworth-Heinemann, Boston, pp. 179–207 (1993).

Tavare, Narayan S., *Industrial Crystallization: Process Simulation Analysis and Design*, Plenum Press, New York (1995).

Van de Hulst, H. C., *Light Scattering by Small Particles*, Wiley, New York (1957).

James B. Rawlings and Daniel B. Patience
Dept. of Chemical Engineering
University of Wisconsin-Madison
Madison, WI 53706